

# Turbulent convection at very high Rayleigh numbers

J. J. Niemela\*, L. Skrbek\*, K. R. Sreenivasan\*† & R. J. Donnelly\*

\*Cryogenic Helium Turbulence Laboratory, Department of Physics, University of Oregon, Eugene, Oregon 97403, USA

†Mason Laboratory, Yale University, New Haven, Connecticut 06520-8286, USA

**Turbulent convection occurs when the Rayleigh number (Ra)—which quantifies the relative magnitude of thermal driving to dissipative forces in the fluid motion—becomes sufficiently high. Although many theoretical and experimental studies of turbulent convection exist, the basic properties of heat transport remain unclear. One important question concerns the existence of an asymptotic regime that is supposed to occur at very high Ra. Theory predicts that in such a state the Nusselt number (Nu), representing the global heat transport, should scale as  $Nu \propto Ra^\beta$  with  $\beta = 1/2$ . Here we investigate thermal transport over eleven orders of magnitude of the Rayleigh number ( $10^6 \leq Ra \leq 10^7$ ), using cryogenic helium gas as the working fluid. Our data, over the entire range of Ra, can be described to the lowest order by a single power-law with scaling exponent  $\beta$  close to 0.31. In particular, we find no evidence for a transition to the  $Ra^{1/2}$  regime. We also study the variation of internal temperature fluctuations with Ra, and probe velocity statistics indirectly.**

Turbulent thermal convection is ubiquitous<sup>1,2</sup> in nature and technology, and serves important and diverse purposes. For instance, it augments radiative heat transport in stars, accomplishes the warming of the atmosphere and the mixing of the oceans, and enhances heat transport in solar heaters and electronic assemblies. A paradigm of convection is the unstable motion of a fluid layer confined between two horizontal flat plates, the bottom plate being hotter than the top. For a Newtonian fluid, the dynamical state of convection is governed by the Rayleigh number  $Ra \equiv g\alpha\Delta TL^3\nu\kappa$  and the Prandtl number  $Pr \equiv \nu/\kappa$ . Here  $g$  is the acceleration due to gravity,  $\Delta T$  is the vertical temperature difference across the fluid layer of height  $L$ , and  $\alpha$ ,  $\nu$  and  $\kappa$  are, respectively, the thermal expansion coefficient, kinematic viscosity and thermal diffusivity of the fluid. In a finite system with a lateral size  $D$ , the aspect ratio,  $\Gamma \equiv D/L$ , could also be a relevant parameter. Turbulent convection sets in at large Ra. The Rayleigh number is of the order of  $10^{20}$  in the ocean and  $10^{23}$  in the outer part of the Sun.

Here we examine the basic properties of heat transport by performing measurements over a very large range of Ra ( $10^6 \leq Ra \leq 10^{17}$ ). We determine the Rayleigh number scaling with far less ambiguity than before and comment on recent claims about the ‘asymptotic’ state of convection; we also report basic data on the statistics of temperature and velocity fluctuations.

## A few basic questions

To understand the importance of experiments over a large Rayleigh number range, consider the Nusselt number, Nu, which is the non-dimensional ratio of the measured heat flux to the conductive heat flux allowed for the same temperature difference between top and bottom plates. Simple scaling arguments and increasingly accurate experiments have suggested that  $Nu \propto Ra^\beta$ . Dimensional reasoning<sup>3</sup> and marginal stability arguments<sup>4</sup> yield  $\beta = 1/3$ . Early experiments were indeed consistent with this expectation. It is now thought that the exponent in those experiments could not have been determined with adequate accuracy because the Rayleigh number range was modest by today’s standards. In fact, the highest Ra attainable in an apparatus of a given size is usually quite limited for a fluid such as water. A particular limitation is that the allowable temperature difference between the top and bottom plates is constrained—if experiments have to make contact with the theory—by the requirement that the fluid properties at the two plates must not be very different; this is the so-called Boussinesq approximation. A more extensive range of Ra was obtained<sup>5</sup> by exploiting the properties of

cryogenic helium gas near its critical point,  $T \approx 5.2$  K and  $p \approx 2.23$  bar. Some researchers<sup>6–9</sup> have taken advantage of this fluid, and obtained Rayleigh numbers up to  $10^{14}$ . Other experiments<sup>10–14</sup> have emphasized several different aspects of the problem.

The Libchaber experiments at larger aspect ratio found  $\beta \approx 2/7$  instead of  $1/3$ , and encouraged the development of alternative scaling theories<sup>8,15,16</sup>; however, the latest experiments<sup>13,14</sup> are not inconsistent with  $1/3$ . Further, even at the highest Ra, the experiments of refs 7,13 and 14 show no tendency towards the so-called asymptotic regime<sup>17</sup>, presumed to be valid for very high Ra (see refs 18 and 19 for upper-bound theories). The asymptotic regime is presumed to occur when the small-scale turbulence generated by the large-eddy shear penetrates even the thinnest conductive layers near the wall, and corresponds to  $\beta = 1/2$  (perhaps with non-trivial logarithmic corrections).

Recently, convection experiments<sup>7</sup> were repeated<sup>9</sup> using cryogenic helium gas in a smaller cell ( $L = 20$  cm) for the same aspect ratio as ref. 7, and reported a continual increase in  $\beta$  beyond  $Ra \approx 10^{11}$ , reaching about 0.4 at  $Ra \approx 10^{14}$ . Chavanne *et al.*<sup>9</sup> interpreted this change as the transition to the asymptotic regime. The Rayleigh number in their experiment was no higher than in refs 7,13 and 14, and so the difference is remarkable. To complicate matters further, others<sup>12</sup> found no tendency towards this asymptotic state in their

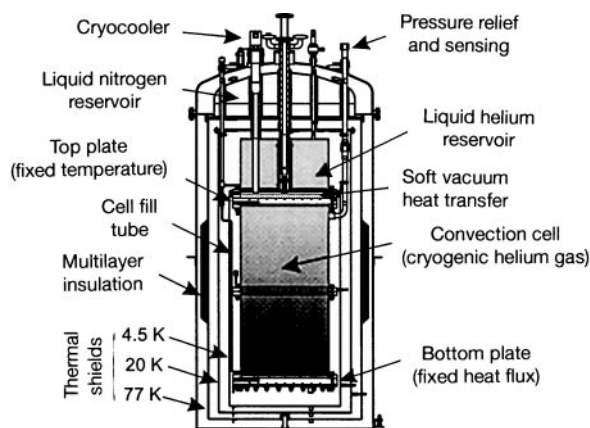


**Figure 1** A schematic view of the experimental apparatus. The working fluid is contained in a cylindrical volume, 1 m high and 0.5 m in diameter.

mercury experiments. Finally, a recent theoretical study<sup>2</sup> has suggested that the  $Nu$ – $Ra$  relation does not follow a strict power-law. At least three questions arise: (1) Does a power law exist? (2) If so, what is the value of  $\beta$ ? (3) Does the asymptotic state exist? Similar questions of fundamental importance can be raised about the properties of fluctuating quantities as well<sup>1</sup>.

### Extending the dynamic range

To address these and other questions, experiments with the highest possible Rayleigh number and the largest possible dynamic range are needed. Here, we report data from such an experiment: heat transport and interior temperature fluctuations are measured in a one-metre Rayleigh–Benard cell over 11 decades of the Rayleigh number between  $10^6$  and  $10^{17}$ . We retained the aspect ratio at 1/2 in order to compare directly with experiments mentioned earlier. The working fluid was cryogenic helium gas in the temperature and pressure ranges of  $4.3\text{ K} < T < 6\text{ K}$  and  $0.1\text{ mbar} < P < 3\text{ bar}$ . Given the relatively large height of our cell (large  $L$ ), we could substantially surpass previous Rayleigh numbers without relying on the divergence of the fluid properties near the critical point, and avoid non-Boussinesq effects.

The apparatus is sketched in Fig. 1. The helium gas was contained between two copper plates, 0.5 m in diameter and 0.038 m in thickness, separated by a thin-wall stainless steel cylinder. The copper was OFHC (oxygen free high conductivity) annealed and had a thermal conductivity of about  $2\text{ kW m}^{-1}\text{K}^{-1}$  at a temperature of 5 K. The surface finish was better than  $10\text{ }\mu\text{m}$ . Specially designed thin metal film heaters were attached to the back side of each copper plate by dilute varnish (GE 7031) and ‘sandwiched’ by an additional thin copper plate of 0.16 cm thickness. The space just above the top plate of the cell was filled with helium gas and served as an adjustable and distributed thermal link between the experiment and the cold

helium reservoir. Three radiation shields surrounded the experimental chamber. A constant heat flux occurred at the bottom plate (and allowed it to attain constant temperature in the steady state), while the top plate was held at a constant temperature by means of a resistance bridge and servo. The standard deviation of the averaged top-plate temperature was typically 0.01 mK.

Calibrated germanium resistance thermometers (Lake Shore Cryotronics, Inc.) measured the average temperature of the plates and were embedded at a distance one-half the radius from the centre at several azimuthal positions. Thirteen small semiconductor probes were placed in the cell interior to measure temperature fluctuations. These were small neutron-transmutation-doped germanium crystal cubes (TRI, Inc.) of side 0.025 cm, with brass leads of diameter 0.0025 cm attached, and had nearly identical temperature sensitivities. Five of them were placed along orthogonal axes in the geometric centre of the cell with a minimum spacing of 3 mm; the remainder were placed in pairs near the sidewall (10–25 mm distance from the wall) at the half-height of the cell with vertical separations of either 3 mm or 25 mm.

The heat input to the bottom plate was measured by a four-wire technique and had an accuracy of better than 100 p.p.m. The pressure of the gas within the cell was measured using a Baratron 390 transducer, with an absolute accuracy of 0.1%, for pressures up to 1 bar. A Texas Instruments Bourdon Tube Gauge was used for pressures between 1 and 3 bar, using the Baratron gauge to monitor the atmospheric reference pressure. These instruments agreed within 0.3% at 1 bar. The adjustment of  $Ra$  was achieved through changes in the gas density, operating temperature, and applied heat flux. The operating temperature, or mean temperature  $T_m$  of the cell, defined as the average of the top and bottom plate temperatures, was used in evaluating all properties of the fluid. Its value was close to that of either plate, as the temperature differences resulting from the applied heat flux to the lower plate were relatively small, typically of the order of 100 mK. In fact, small changes in  $Ra$  were made most conveniently by changing the power  $\dot{Q}$  applied to the bottom plate, while holding the top-plate temperature and gas

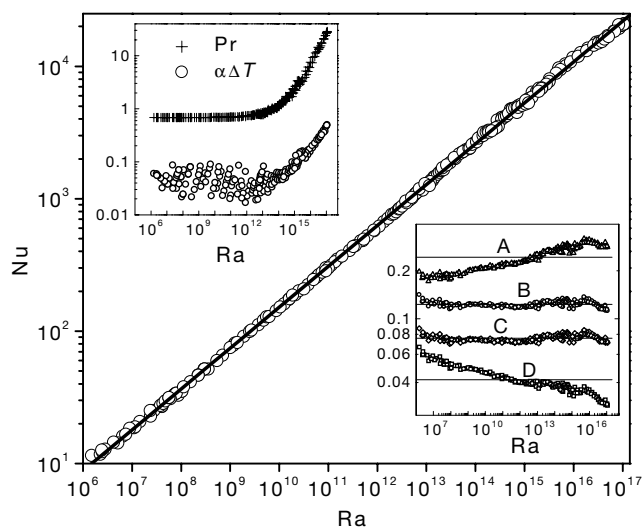


**Figure 2** Log–log plot of the Nusselt number ( $Nu$ ) versus Rayleigh number ( $Ra$ ). The line through the data is the least-squares fit over the entire  $Ra$  range, and represents  $Nu = 0.124 Ra^{0.309}$ . Locally, the power-law exponent shows a modest change with  $Ra$ , but these high-order effects are not considered here. Bottom right inset, the compensated plot B represents  $Nu/Ra^{0.309}$  and confirms this relation. The ‘mean field theory’ for optimal heat transport for a single mode also fits the entire range of the data if the prefactor is chosen to be 0.0587 (plot C). When  $Nu$  is normalized by the 2/7th power of  $Ra$  (plot A) or by the 1/3rd power of  $Ra$  (plot D), the resulting plots are not constant in  $Ra$ , suggesting that neither exponent is correct. Top left inset, the upper set of data (crosses) shows the variation of the Prandtl number. The best fit to the  $Nu$ – $Ra$  data for  $Ra < 10^{13}$ , where  $Pr$  is a constant of 0.7, gives only a slightly different exponent of 0.308. The lower set of data (circles) is  $\alpha\Delta T$ , this product being a measure of the non-Boussinesq effects. For all but the last dozen or so of the data at the highest  $Ra$ ,  $\alpha\Delta T < 0.2$ . This is considered to be sufficiently small.

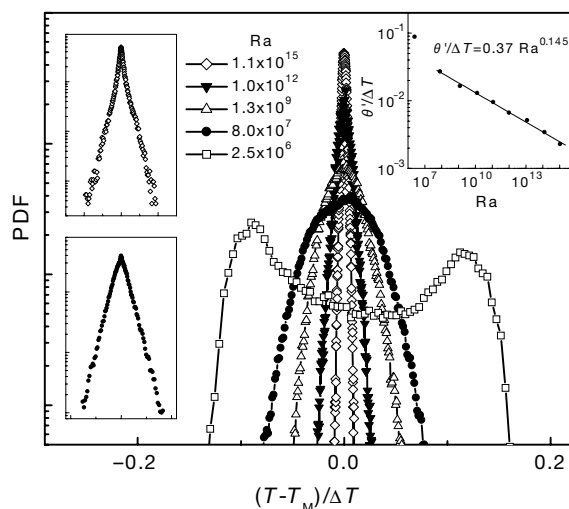


**Figure 3** The probability density function (PDF) of the temperature fluctuations in the centre of the cell measured at different  $Ra$  as indicated. At the lowest  $Ra$ , the PDF retains a memory of the hot and cold temperatures. Bottom left inset, the PDF for  $Ra = 8.7 \times 10^7$  is gaussian, where the log of the PDF is plotted against the squared temperature difference from the mean. Top left inset, the PDF similarly plotted for  $Ra = 1.1 \times 10^{15}$ , where it takes the form of a stretched exponential (with a stretching factor of 1.5). The temperature scale ranges between  $-10^{-4}$  and  $+10^{-4}$  (top left inset) and between  $-0.01$  and  $+0.01$  (bottom left inset). Top right inset, the ratio of the root-mean-square temperature fluctuation  $\theta'$  to the mean temperature difference  $\Delta T$  across the bottom and top plates, as a function of  $Ra$ .  $T_m$ , mean temperature of the cell.

density constant. The Rayleigh number could also be increased for a given applied heat flux and gas density by setting the (controlled) top-plate temperature closer to the critical temperature of the gas. This was done in a few instances. The diverging gas properties led to higher Ra for nominally constant temperature differences. Coarse control of Ra was achieved by changing the density of the sample gas; this required transferring helium between the main helium reservoir and the cell through a cryogenic valve and filter. The gas density, determined from the measured pressure and mean temperature, varied between  $2 \times 10^{-6} \text{ g cm}^{-3}$  to  $0.076 \text{ g cm}^{-3}$  in these experiments.

Over most of the range of Ra, the waiting times after a change in  $\dot{Q}$  were of the order of an hour; the more precise value depended on the strength of the convective flow and the total heat capacity of enclosed gas. In practice, it was determined individually from the continuous time record of the plate temperatures. From the exponential approach to equilibrium in the bottom-plate temperature, a minimum of five characteristic times was allowed to elapse before data were taken. Each plate temperature was then averaged several times for up to 30 minutes. The Nusselt number was calculated from the measured temperature difference  $\Delta T$  and the applied power  $\dot{Q}$ , taking into account corrections for heat conduction through the confining stainless steel walls of the cell and the adiabatic temperature gradient,  $\Delta T_{\text{ad}} = g\alpha L T_m / C_p$ , where  $C_p$  is the heat capacity at constant pressure. Values of  $\Delta T_{\text{ad}}$  were generally of order 2–3 mK, and were subtracted from the measured temperature difference before evaluating Ra and Nu.

Temperature fluctuations were measured from the changing resistance of the small germanium sensors in the flow, which formed one arm of an audio-frequency resistance bridge operated off-balance with phase-sensitive detection. Each time series typically contained  $2^{19}$  data points, corresponding to about 5 hours of real time.

### Heat transport scaling

Figure 2 shows Nu as a function of Ra in a log–log plot for  $10^6 \leq \text{Ra} \leq 10^{17}$ . This extensive dynamic range allows us to draw several useful conclusions. First, over the entire range of Rayleigh numbers, a single power law fits the data well to the lowest order, as shown by the solid line through the data. The fit yields  $\text{Nu} = 0.124 \text{ Ra}^{0.309 \pm 0.0043}$ . Plotting  $\text{Nu} - 1$  instead of Nu, or plotting Nu or  $\text{Nu} - 1$  against  $\text{Ra} - \text{Ra}_{\text{cr}}$  (where  $\text{Ra}_{\text{cr}}$  is the critical Rayleigh

number), does not materially affect this conclusion. Second, it appears that  $\beta$  values of 1/3 as well as 2/7 are ruled out, as demonstrated by the compensated plots in the bottom right inset to Fig. 2.

It is important to note, however, that the precise value of  $\beta$  depends on the helium gas properties used to compute Ra and Nu. A significant part of the difference between the present value of  $\beta$  and that of ref. 7 appears to be due to such differences—most notably in the thermal conductivity. The gas properties used here were obtained from software (Cryodata Inc.) incorporating NIST-12 Standard Reference Database code, adopted in 1992 as the international standard for helium properties. This software was especially modified for increased accuracy near the critical point<sup>20</sup>. The properties obtained from the NIST-12 code differ appreciably from the older NBS values<sup>21</sup> used by ref. 7. For comparison, we have recomputed their data with the updated gas properties as well as adiabatic corrections, and found the best fit for  $\text{Ra} > 5 \times 10^7$  to be  $\text{Nu} = 0.146 \text{ Ra}^{0.299}$ . The exponent  $\beta$  in the SF<sub>6</sub> measurements of ref. 13 is  $0.3 \pm 0.03$ . Although that mean value is consistent with the present result, the relatively larger uncertainty cannot rule out either 2/7 or 1/3.

There is no fully fledged theory that predicts the observed trend correctly, but a ‘mean-field’ result culled from the works of Howard, Roberts, Stewartson, and Herring (see refs 22, 23 for a summary) has the correct functional form. This result pertains to a single-mode solution of the convection just past the critical Rayleigh number in which the wavenumber of the weakly nonlinear mode is determined by maximizing the heat transport. That result gives  $\text{Nu} = 0.24 (\text{Ra}^{3/2} \ln \text{Ra}^{3/2})^{1/5}$ , with additional log–log terms in the next order. The inset shows that this expression with an empirically adjusted prefactor of 0.0587 fits the entire range of Ra very well. Whether this remarkable agreement is more than accidental remains to be seen. An elementary one-dimensional theory (B. Dubrulle, personal communication) also yields an exponent compatible with the present measurements.

There are slight departures from the power law in the last two or so decades of Ra. Whether they are due to logarithmic corrections, modest non-Boussinesq effects or Prandtl number variability is not

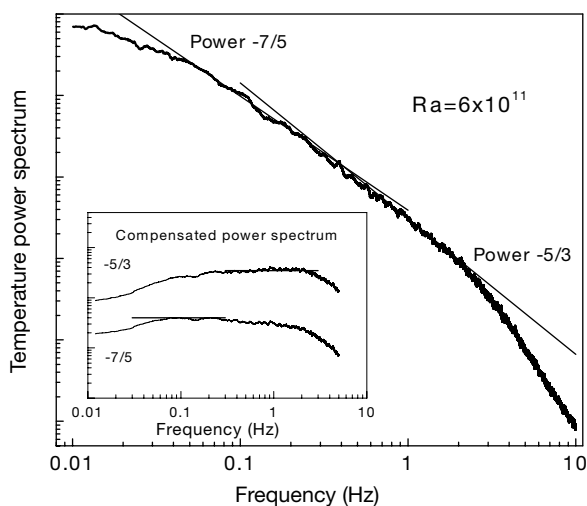


**Figure 4** The power spectral density (PSD) of the temperature fluctuations in the cell measured at  $\text{Ra} = 6 \times 10^{11}$ . The PSD has a roll-off rate of 7/5 for low frequencies where Bolgiano scaling seems appropriate, whereas for higher frequencies, the classical Obukhov–Corrsin scaling appears to hold. Inset, the PSD compensated for the roll-off exponents of 7/5 and 5/3. The crossover position is determined by the magnitude of the Bolgiano length scale.

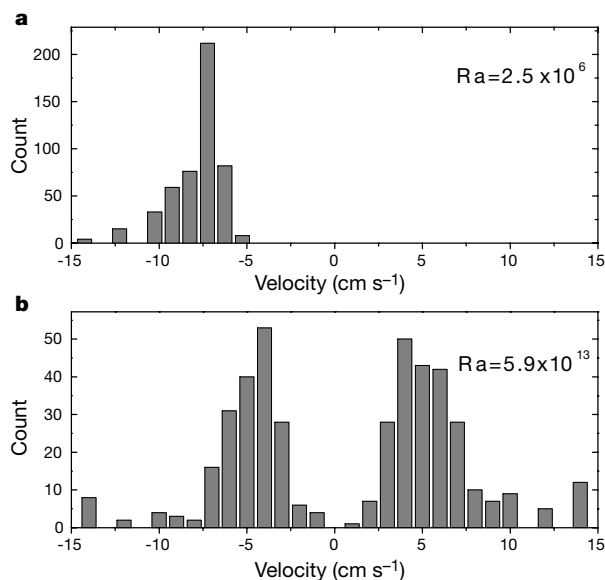


**Figure 5** A rough measure of the large-scale velocity in the cell. The method of obtaining the data is described in the text. For  $\text{Ra} = 2.5 \times 10^6$ , the velocity is unidirectional over the duration of the experiment, and probably reflects a well-maintained large-scale circulation. At higher Rayleigh numbers, the motion can be in both directions, but cannot be represented simply by an oscillatory circulation. It may more accurately represent the large-scale motion upon which small-scale fluctuations are superimposed.

completely clear. The non-Boussinesq effects appear to be small because the product  $\alpha\Delta T$  (circles in the left inset of Fig. 2) is less than 0.2 for all but the last dozen or so data points—this being an empirical criterion for validity of the Boussinesq approximation<sup>24</sup>. The Prandtl number is a constant at least up to  $Ra \approx 10^{13}$  (crosses in the left inset of Fig. 2), and the fit to the  $Ra$ – $Nu$  data in that region yields a  $\beta$  that differs from 0.309 only in the third decimal place. Thus, the Prandtl number effect on the  $Nu$  behaviour appears to be small as well. If we attribute the slight droop of  $Nu$  below the power-law fit in the last three or so decades of  $Ra$  entirely to Prandtl number effects, we can fit that effect by  $Pr^{-1/7}$  (consistent with refs 13 and 15). (This is different in sign from the Prandtl number effects for  $Pr = 0.1$ , for which available numerical and experimental data<sup>25</sup> at  $Ra \approx 6 \times 10^5$  suggest that  $Nu \propto Pr^{0.14}$ .)

### Temperature and velocity fluctuations

The apparent uniqueness of the power-law that characterizes—at least to first order—the  $Nu$ – $Ra$  relation does not imply that the dynamical behaviour of the heat transport is similarly unique. Even the simplest statistics of the temperature fluctuation  $\theta$ , such as its probability density function (PDF) and power spectral density (PSD), undergo drastic changes with Rayleigh number, as has already been noted by other workers (for example, see ref. 7). A sample of these changes is shown in Fig. 3. At the centre of the cell, the PDF of  $\theta$  is bimodal at  $Ra = 2.5 \times 10^6$ , suggesting that the top- and bottom-plate temperatures are not fully mixed. The mixing is essentially complete by  $Ra = 8.7 \times 10^7$ , where the PDF is almost gaussian (see bottom left inset in Fig. 3, where PDFs are plotted against the square of the temperature difference from the mean). The PDFs at higher Rayleigh numbers, say  $Ra \geq 10^{10}$ , show a stretched exponential behaviour (top left inset in Fig. 3). The asymptotic state of the temperature PDF is thus not gaussian. The inset on the right shows that the root-mean-square fluctuation  $\theta'$  of  $\theta$  follows the relation  $\theta'/\Delta T = 0.37 Ra^{-0.145}$ , quite close to the result of ref. 7. The PDF at any off-centre position in the cell is much more complex, and will not be discussed here.

Figure 4 shows one feature of the power spectral density of  $\theta$ . At low frequencies, the roll-off rate is 7/5, consistent with Bolgiano's theory<sup>26</sup>. At higher frequencies, one observes the classical Obukhov–Corrsin scaling with the 5/3 roll-off rate<sup>27</sup>. This is particularly clear from the compensated spectra plotted in the inset. The cross-over between the two power-laws occurs at the so-called Bolgiano scale. We cannot reliably determine the Bolgiano scale as a function of  $Ra$ , but the preliminary data at other Rayleigh numbers are consistent with this picture.

We have not measured the velocity fluctuations in the cell directly. However, following ref. 7, we have estimated the velocity by correlating a temperature signal from one bolometer with that from another situated a known distance away, the latter with a time delay that maximizes the correlation. The ratio of the separation distance to this delay time gives an estimate of the velocity along the axis separating the two bolometers. The correlation is obtained by averaging over an intermediate timescale  $\tau$  that is large compared to the digital sampling interval but small compared to the large-scale turnover in the cell. The velocity estimates so obtained are thus coarse-grained averages over the duration  $\tau$ . If the flow speed is unidirectional, the delay time needed for maximizing the correlation will be of one sign; otherwise, it will change sign at intervals.

For Rayleigh numbers of about  $2.5 \times 10^6$ , the estimated flow speed is shown in Fig. 5a. The most probable velocity, corresponding to the peak in the histogram, is of the order  $7 \text{ cm s}^{-1}$ ; the spread represents the fluctuations around this most probable value. The mean velocity is unidirectional over the duration of the experiment (about 6 hours of real time). Thus, a large-scale circulation—albeit a wobbly one—appears to survive at Rayleigh numbers of this order. At higher Rayleigh numbers of the order  $6 \times 10^{13}$ , the velocity

histogram assumes a bimodal shape shown in Fig. 5b, suggesting that the large-scale flow is no longer unidirectional over the experimental duration, but may change sign frequently. In reality, even this bimodality is an artefact of the finiteness of  $\tau$ ; the use of a smaller  $\tau$  fills the gap between the two modes of the histogram.

There has been considerable speculation on the effect of the large-scale circulation on the experimentally observed  $Nu$ – $Ra$  scaling<sup>1,2,7–11,28</sup>. A reasonable approximation to a steady mean flow in the cell is observed only at the low end of the Rayleigh number range. At higher Rayleigh numbers, the motion is at least as often in one direction as another; it is more like a weak large-scale motion on which are superimposed small-scale velocities. It is not clear how this conclusion translates to convection cells of larger aspect ratio<sup>29</sup>. Our future goals include the direct measurement of the velocity and a better understanding of the effects of variable Prandtl number and aspect ratio. □

Received 25 August 1999; accepted 9 February 2000.

- Siggia, E. D. High Rayleigh number convection. *Annu. Rev. Fluid Mech.* **26**, 137–168 (1994).
- Grossmann, S. & Lohse, D. Scaling in thermal convection: A unifying theory. *J. Fluid Mech.* (in the press).
- Priestley, C. H. B. *Turbulent Transfer in the Lower Atmosphere* (Univ. Chicago Press, Chicago, 1959).
- Malkus, W. V. R. Heat transport and spectrum of thermal turbulence. *Proc. R. Soc. Lond. A* **225**, 196–212 (1954).
- Threlfall, D. C. Free convection in low-temperature gaseous helium. *J. Fluid Mech.* **67**, 17–28 (1975).
- Wu, X.-Z. & Libchaber, A. Scaling relations in thermal turbulence: the aspect ratio dependence. *Phys. Rev. A* **45**, 842–845 (1992).
- Wu, X.-Z. *Along a Road to Developed Turbulence: Free Thermal Convection in Low Temperature Helium Gas* PhD thesis, Univ. Chicago (1991).
- Castaing, B. *et al.* Scaling of hard thermal turbulence in Rayleigh-Benard convection. *J. Fluid Mech.* **204**, 1–29 (1989).
- Chavanne, X. *et al.* Observation of the ultimate regime in Rayleigh-Benard convection. *Phys. Rev. Lett.* **79**, 3648–3651 (1997).
- Shen, Y., Tong, P. & Xia, K.-Q. Turbulent convection over rough surfaces. *Phys. Rev. Lett.* **76**, 908–911 (1996).
- Cioni, S., Ciliberto, S. & Sommeria, J. Strongly turbulent Rayleigh-Benard convection in mercury: comparison with results at moderate Prandtl number. *J. Fluid Mech.* **335**, 111–140 (1997).
- Glazier, J. A., Segawa, T., Naert, A. & Sano, M. Evidence against 'ultrahard' thermal turbulence at very high Rayleigh numbers. *Nature* **398**, 307–310 (1999).
- Ashkenazi, S. & Steinberg, V. High Rayleigh number turbulent convection in a gas near the gas-liquid critical point. *Phys. Rev. Lett.* **83**, 3641–3644 (1999).
- Ashkenazi, S. & Steinberg, V. Spectra and statistics of velocity and temperature fluctuations in turbulent convection. *Phys. Rev. Lett.* **83**, 4760–4763 (1999).
- Shraiman, B. I. & Siggia, E. D. Heat transport in high-Rayleigh-number convection. *Phys. Rev. A* **42**, 3650–3653 (1990).
- She, Z.-S. On the scaling laws of thermal turbulent convection. *Phys. Fluids A* **1**, 911–913 (1989).
- Kraichnan, R. H. Turbulent thermal convection at arbitrary Prandtl number. *Phys. Fluids* **5**, 1374–1389 (1962).
- Howard, L. N. Heat transport by turbulent convection. *J. Fluid Mech.* **17**, 405–432 (1963).
- Constantin, P. & Doering, C. Infinite Prandtl number convection. *J. Stat. Phys.* **94**, 159–172 (1999).
- Arp, V. D. & McCarty, R. D. *The Properties Of Critical Helium Gas* Technical Report, Univ. Oregon (1998).
- McCarty, R. D. *Thermophysical Properties of Helium-4 from 2 to 1500 K with Pressures to 1000 Atmospheres* (Technical Note 631, National Bureau of Standards, Gaithersburg, Maryland, 1972).
- Toomre, J., Gough, D. O. & Spiegel, E. A. Numerical solution of single-mode convection equation. *J. Fluid Mech.* **79**, 1–31 (1977).
- Busse, F. H. Nonlinear properties of thermal convection. *Rep. Prog. Phys.* **41**, 1930–1967 (1978).
- Chavanne, X. *et al.* High Rayleigh number convection with gaseous helium at low temperature. *J. Low Temp. Phys.* **104**, 109–129 (1996).
- Verzicco, R. & Camussi, R. in *Advances in Turbulence VII* (ed. Frisch, U.) 399–402 (Kluwer Academic, Dordrecht, 1998).
- Bolgiano, R. Jr Turbulent spectra in a stably stratified atmosphere. *J. Geophys. Res.* **64**, 2226–2229 (1959).
- Monin, A. S. & Yaglom, A. M. *Statistical Fluid Mechanics* Vol. 2 (M.I.T Press, Cambridge, Massachusetts, 1975).
- Ciliberto, S., Cioni, S. & Laroche, C. Large scale flow properties of turbulent thermal convection. *Phys. E* **54**, 5901–5905 (1996).
- Krishnamurti, R. & Howard, L. N. Large scale flow generation in turbulent convection. *Proc. Natl Acad. Sci. USA* **78**, 1981–1985 (1981).

### Acknowledgements

We thank M. McAshan for his assistance in the design of the cryostat, and many colleagues for useful discussions. This research was supported by the US National Science Foundation.

Correspondence and requests for materials should be addressed to R. J. D. (e-mail: russ@vortex.uoregon.edu).